The use of wrist EMG increases the PPG Heart Rate accuracy in smartwatches

Severi Friman, Antti Vehkaoja, Jose Maria Perez-Macias

***Abstract*—The impact of tissue movements on the accuracy of heart rate (HR) estimates is a challenge in today's wearable technology. Tissue movements are caused by muscle activity that modifies the optical path of the reflectance photoplethysmography (PPG), leading to motion artifacts (MA) that mask the true HR. This kind of MA is not always detected using accelerometers (ACC).**

In this study, we propose a method to increase the PPG HR accuracy of a wristwatch using wrist surface electromyogram (EMG) and ACC using spectrum subtraction algorithms.

We collected the wrist EMG, wristwatch PPG, ACC data, and the ECG from nine subjects. Data were recorded during four frequent hand movements and three activities (weightlifting and running/walking with and without holding a racket). The added value of the EMG was studied. Visual results indicate that wrist EMG correlates well with the MA seen in the PPG signal and provides additional information over the typically used ACC data. Our analysis showed that the proposed artifact removal method using EMG and ACC decreases the HR estimation error on average by 49% compared to only ACC. Our results showed that wrist EMG contains complementary information on the PPG artifacts and offers a novel signal modality for improving optical HR estimation accuracy in smartwatches.

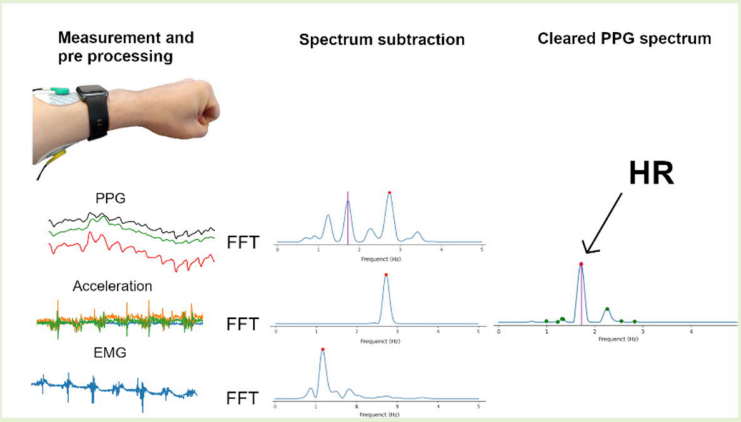

***Index Terms*—Electromyogram, Photoplethysmogram, Tissue Movement, Heart Rate, Motion Artifacts**

I. INTRODUCTION

HEART rate (HR) is one of the most monitored vital signs. It provides the user with relevant information about health status and their level of physical stress. In a medical context, unexpected HR patterns might indicate changes in patient's health status [1]. From a consumer perspective, HR can inform the monitored person about their exercise intensity, mental or physical stress and recovery. An accurate and robust measure of HR is thus important for health monitoring.

Electrocardiography is a routine clinical method to measure the heart's electrical activity. It is measured with multiple electrodes placed on the skin. The electrocardiogram (ECG) is considered the most accurate method for HR measurement. However, its use for long term monitoring in everyday applications is uncomfortable and difficult to use [2].

Photoplehtysmogram (PPG) uses an emitting light source and a receptor to measure heart activity. As the heart pumps blood to the tissue, the amount of detected light decreases [3] and the modulation of the detected light can be used to estimate the HR.

PPG-based HR measurement devices enable more comfortable use and user-friendly form factors, such as smartwatches [4]. However, PPG based HR measurement devices are vulnerable to movement artifacts (MA), causing distortions in the recorded signals. Wrist PPG is especially sensitive to body movement artifacts making HR measurement difficult. The use of the accelerometer to remove these MAs has been extensively researched [5]–[12]. Its use is considered efficient in removing the artifacts caused by larger movements.

Tissue movement artifacts are a less researched artifact type referred to as micromotion artifacts [13], [14]. This type of artifact originates from small movements caused by skeletal muscle contractions, causing the tissue under the PPG sensor to move. This movement causes changes in the contact force or coupling between the sensor and the skin tissue and modifies the optical path. Artifacts caused by this type of tissue

S. Friman is with Huawei technologies Oy (Finland) CO Ltd, as a testing and processing engineer. (e-mail: severi.friman1@huawei.com).

A. Vehkaoja is with the Faculty of medicine and Health Technology, Tampere University, Tampere, Finland (e-mail: antti.vehkaoja@tuni.fi).

J.Perez-Macias was with Huawei Technologies Oy (Finland) CO Ltd, and currently is with Faculty of Medicine and Health Technology, Tampere , Tampere, Finland (e-mail: jose.perez-macias@tuni.fi).

movement cannot be detected reliably using the acceleration. Previous research suggests that tissue movement artifacts require additional reference signals and methods to improve the HR [13]–[16].

I. Related work

Tissue movement artifacts are a known issue in wrist PPG wearables. These are caused by muscle activations from hand and finger movements that result in the movement of muscles and tendons.

To our knowledge, few studies are addressing the tissue movement artifact problem [13]–[16]. Zhang et *al.* used the infrared (IR) wavelength as a motion reference [13]. The authors used support vector machines to detect and remove low-quality data. The higher sensitivity of IR wavelengths to this type of artifacts allowed the authors to use this IR PPG as a movement reference and use this reference in the spectrum subtraction algorithm of the green PPG signal. The proposed algorithm reduced the average errors of HR from 4.3, 3.0 and 3.8 BPM to 0.6, 1.0 and 2.1 BPM in periodic, random, and continuous non-periodic motion situations, respectively.

In another study by Ferreira et al., ambient light measured by the PPG sensor photodetector was used as a tissue movement reference. The authors used adaptive filtering (least mean squares algorithm; LMS) to filter the PPG signal. They reported that their solution had +1.4/-2.0 BPM limits of agreement compared to the ECG-based HR.

Lee et *al.* used a pressure signal from a piezoelectric transducer as a reference and used spectrum subtraction to compensate for these movements [16]. Their results demonstrated that the pressure sensor transducer placed on the wrist could detect repetitive finger and hand movements, whereas the accelerometer was not able to detect them. In their approach, the mean absolute error (MAE) and standard deviation (SD) of the HR decreased from 3.75 ± 2.96 to 1.58 ± 2.96 BPM during treadmill running. They attributed this improvement to the contraction of the forearm muscles during running in some subjects. The principle of subtracting the acceleration spectrum from PPG spectrum in order to enhance HR frequencies has been earlier studied with good results. Salehizadeh et al. [17] applied this approach on a 33-person dataset consisting of running exercises and achieved an average error of 1.86 BPM. Time frequency spectrum subtraction was used also in study by Kong et al. [18] in which HR was estimated from wristwatch and forehead PPG data of 22 people during treadmill exercise. They achieved an average absolute error of 2.94 BPM, which is less accurate than results by Salehizadeh et al., but they argued that it is the cost for better temporal resolution of the estimates. These solutions demonstrate the potentials of artifact removal by spectral subtractions, but the effectiveness in cases involving tissue movement artifacts requires additional movement references like in the study by Lee et. al.

Silverio et *al.* [14] used forearm EMG as their tissue movement reference. They performed continuous wavelet transform subtraction and adaptive LMS filtering to correct the corrupted PPG signals from finger movements and hand squeezing. Their results showed that the spectrum subtraction with the EMG signal increased the Signal to Noise Ratio (SNR) of the PPG and increased the correlation with a resting PPG signal. Although the study did not evaluate the impact of the increased SNR in terms of HR accuracy, they demonstrated the use of EMG as a noise reference signal.

As a follow-up to the study by Silverio et *al.*, in the present study, the use of wrist surface EMG (S-EMG)—instead of forearm EMG—to detect and reject tissue movement artifacts were evaluated. The wrist S-EMG was chosen instead of forearm EMG, as it would be easier to implement on wrist worn devices. Also, unlike Silverio et al., the present study aims at investigating the use of S-EMG during movement tasks, better demonstrating the performance during exercise. We evaluated its efficacy using typical HR accuracy measures during typical hand movements and activities using EMG and acceleration. The principles of spectrum subtraction algorithms demonstrated by Lee, Salehizadeh and Kong et al. are used to implement HR estimation algorithms using both wrist acceleration and wrist EMG as movement artifact reference signals.

II. Materials and Methods

The study was conducted in Huawei Technologies Finland research center, Helsinki. Subjects were recruited from Huawei Technologies research center using an internal mailing-list, Helsinki. Inclusion criteria included 18–65 years and good health. All volunteers agreed to participate in this research and signed written informed consent. Data processing was performed following a Data Protection Impact Assessment (DPIA) approved by an EU privacy officer. Nine (9) measurement subjects participated in the study. Anthropometric measurements and the background information on participant's physical fitness level were not collected due to limitations of the DPIA used in this study.

A. Measurement setup

An ECG, wrist EMG, wrist acceleration, and reflective wrist PPG were recorded. ECG was recorded as HR reference. To detect hand muscle activations, EMG was measured from the left wrist. The EMG electrodes were placed on the top and bottom sides of the wrist (Fig. 1).

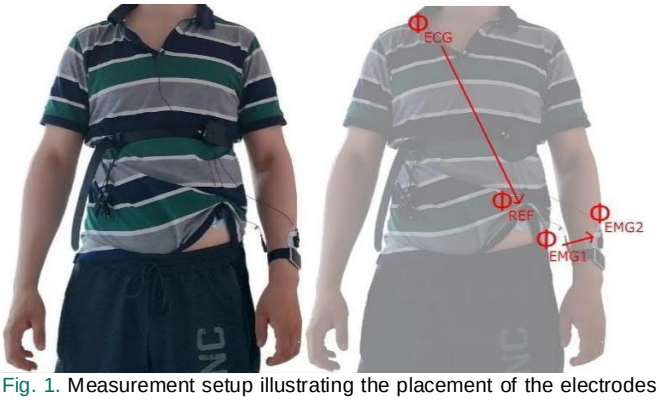

Fig. 1. Measurement setup illustrating the placement of the electrodes and wristwatch.

The ECG and EMG were recorded (sampled at 250 Hz) using a Mentalab Explore (Mentalab, Germany) [19] device using

disposable adhesive gel electrodes (Ambu, Whitesensor 4500M-H) [20]. Before their attachment, the skin was cleaned with an abrasive gel for better electrical coupling. The EMG and ECG were measured using the following electrode configurations:

$$ECG = -(\Phi_{ECG} - \Phi_{REF}) \quad (1)$$

$$EMG = \Phi_{EMG2} - \Phi_{REF} - (\Phi_{EMG1} - \Phi_{REF}) = \Phi_{EMG2} - \Phi_{EMG1} \quad (2)$$

where Φ_{ECG}, Φ_{REF}, Φ_{EMG1}, and Φ_{EMG2} are the electrical potentials in the electrode locations.

A custom-made smartwatch prototype was used to record the PPG and acceleration sampled at 100 Hz. The device was placed one finger from the distal end of the ulnar bone. The green PPG signal was used because of its robustness against MA [21]. ECG and EMG were streamed in real-time to a laptop via Bluetooth® connection, and the PPG and acceleration were recorded using a smartphone.

B. Measurement protocol

The subjects were instructed to perform a series of tasks and activities during the session. The tasks and their descriptions are shown in Table 1. The tasks were designed to contain tissue and/or body movements to study the usefulness of acceleration and/or EMG in individual and combined tasks for artifact removal.

Hand, wrist, and finger activities were included because they represent the most common movements during exercise and sources of artifacts. Other tasks consisting of either hand or finger movements were included to study how well the wrist EMG was able to detect these types of movements. Finally, the remaining tasks contain both tissue and body movement, e.g. hand weightlifting and running with and without a floorball racket in hand.

TABLE I
MOVEMENT TASKS PERFORMED BY THE SUBJECTS. THE DURATION DESCRIBES THE TIMING OF THE PHASES OF EACH TASK AND FREQUENCY RAMPS FOR THE TEMPO.

Task	Duration	Frequency / Pace
hand opening/closing (Sitting, hand on table)	-15s rest -180s repetitions -15s rest	0.5 → 3 → 0.5 Hz (30 → 180 → 30 BPM)
finger movement (Sitting, hand on a table, lifting and lowering individual finger from the tabletop)	-15s rest -20s per finger = 100s repetitions -15s rest	0.5 → 4 → 0.5 Hz (30 → 240 → 30 BPM)
wrist flexion/extension (Sitting, hand on table)	-15s rest -180s repetitions -15s rest	0.5 → 3 → 0.5 Hz (30 → 180 → 30 BPM)
hand squeezing (Sitting, hand on table)	-15s rest -180s repetitions -15s rest	0.5 → 3 → 0.5 Hz (30 → 180 → 30 BPM)
Hand weightlifting (Sitting. biceps flexion)	-15s rest -60s repetitions -15s rest	At start 0.5 Hz Then the subject can do as fast as he/she can
Running / walking with racket in hand (Back and forth a corridor. Racket at the same hand with measurement devices)	-15s rest -120s of walking -120s of running -120s of walking -15 seconds rest	1 → 2 → 1 Hz (60 → 120 → 60 steps / minute)
Running / fast walking (Back and forth a corridor)	-15s rest -120s of walking -120s of running -120s of walking -15s rest	1 → 2 → 1 Hz (60 → 120 → 60 steps / minute)

The tempo of each task was adjusted during the measurement. Subjects were provided with audio-visual cues using a smartphone metronome App to change the tempo. The tempo ranged from 0.5 to 3 Hz and returned to 0.5 Hz using the metronome. These frequency ramps were included to ensure that the artifact frequency overlaps the HR frequency during the measurement. This overlapping is important because, at those time instances, the HR estimation algorithm is most likely to start to follow the artifact frequency.

In addition to a 2-minute resting PPG recording, each measurement consisted of a simultaneous tap on the smartwatch and the EMG electrode for synchronization purposes, 15 seconds of resting PPG followed by the repetitive task.

C. Signal processing pipeline

Data synchronization between the two measurement devices was done by matching the sensor tapping events in the EMG and acceleration signals. The resulting EMG signal was down sampled to 100 Hz to match the PPG and acceleration signals. The average rectified value (ARV) of the resulting signal was calculated similarly to Guo et *al.* [20]:

$$ARV = \frac{1}{N}\sum_{i=1}^{N}|x_i| \quad (3)$$

where N is the number of samples in the window and x_i is the sample at the ith index of the calculation window. An average filter of $N = 15$ was used (150ms). The ARV was then highpass filtered from 0.8 Hz to eliminate the low-frequency components introduced by the absolute averaging window. The formation of ARV from EMG signal is demonstrated in Fig. 2:

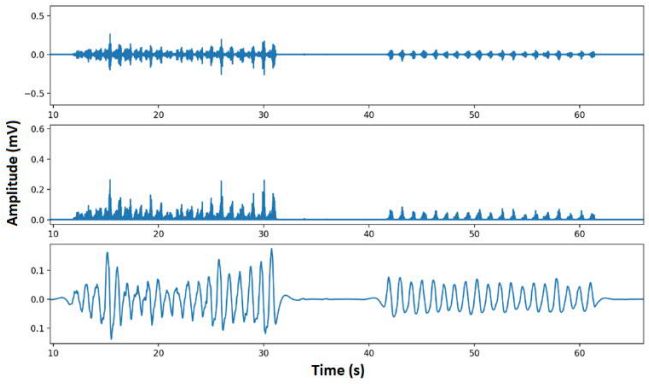

Fig. 2. *Tissue movement signal formation. Top panel: filtered EMG, middle panel: rectified electromyogram (EMG), bottom panel: high pass filtered averaged rectified value (ARV) signal.*

The ARV, acceleration, and PPG signals were filtered using a 4th order band-pass Butterworth IIR filter at cut-off frequencies of 0.8 and 4 Hz, corresponding to an HR of 48 and 240 bpm. This was done to factor out physiologically improbable HR during exercise. The algorithm could easily be modified to support the lower heart rates in resting state. Also, the watch could have different modes for exercise and non-exercise HR. The ECG was filtered with a 0.5 Hz high pass and a 50 Hz notch filter.

After pre-processing, the data were processed using an eight-second window with a six-seconds overlap, which resulted in one HR estimate every two seconds. The ARV, acceleration, and PPG signals spectrum was estimated using a Fast Fourier Transform (FFT) using 12500 zero-padding over the estimation window. Zero padding enables smoother transitions between frequency bins, enabling higher resolution in the HR estimation after the spectrum subtraction algorithm. The resulting frequency resolution was 0.008 Hz or 0.48 BPM time resolution. The spectrums were converted to power and normalized between one and zero. A Hanning window was used prior to the FFT. The FFTs were calculated with a SciPy Python library function [23] that uses Cooley-Tuckey FFT algorithm [24].

The aim of the spectrum subtraction algorithms is to remove the frequency components related to artifacts from the corrupted PPG signal, resulting in a clearer PPG spectrum. The subtracted signals from the PPG frequency spectrum were the acceleration and EMG ARV frequency spectrums. This can be denoted as:

$$P_E \approx P_s - P_r \tag{4}$$

where P_E is the estimation of the clear PPG frequency spectrum after the subtraction of the artifact spectrum from the corrupted PPG spectrum P_s. The artifact spectrum P_r can be divided into EMG and acceleration spectra components.

$$P_E \approx P_s - P_r = \left(\frac{P_s - P_r}{P_s}\right) P_s = W P_s \tag{5}$$

As there are the two artifact components, the weight vector can be denoted as two separate components:

$$P_E \approx \left(\frac{P_s - P_{ACC}}{P_s}\right)\left(\frac{P_s - P_{EMG}}{P_s}\right) P_s = W_{ACC} W_{EMG} P_s \tag{6}$$

By substituting the P_s term from both weights, the equation gets a form of a Wiener filter [23]:

$$P_E \approx= W_{ACC} W_{EMG} P_s = \left(\frac{P_E}{P_E + P_{ACC}}\right)\left(\frac{P_E}{P_E + P_{EMG}}\right) P_s \tag{7}$$

The denominators of the weights can be substituted with the estimate from the previous estimation window $P_E(i-1)$ as the clear PPG spectrums of two consecutive time windows should be close to each other. This leads to the final form of the spectrum subtraction equation:

$$P_E(i) \approx \left(\frac{P_E(i-1)}{P_E(i-1) + P_{ACC}(i)}\right)\left(\frac{P_E(i-1)}{P_E(i-1) + P_{EMG}(i)}\right) P_s(i) \tag{8}$$

The use of the previous window estimate in the next window means that the first estimation window should be a relatively clean PPG. The assumption that the estimation in the previous windows is close to the next (8) can lead to erroneous estimates when fast HR changes occur. Fast HR changes lead to larger differences between two consecutive windows preventing the algorithm from following the HR. To address this problem, the final spectrum estimate is formed as the average of the spectra from Equations 6 and 8. Equation 6 adds up more weight on the more recent heart rate related information in the PPG spectrum, while Equation 8 keeps the focus in the right frequency region. The recursive spectrum subtraction algorithm follows the same principles as in the study by Lee et al. [16], while averaging the spectra from Equations 7 and 9 is a novel adjustment on the algorithm. The result of the spectrum subtraction in a single time window is visualized in Fig. 3.

Prior to the subtraction algorithm, both reference spectra are normalized. In practice, this means that both spectra have the same amplitude and effect in the subtraction algorithm. However, normalization also means that weak signals have the same magnitude of filtering effect as strong signals, which is a potential source of errors in stable measurement conditions when the PPG does not contain any artifacts. In this case, the PPG spectra would be subtracted with movement reference spectra containing non-related movement noise. To address this scenario, a threshold of the power of both signals was used to decide whether the PPG is corrupted with artifacts the PPG should be subject to be corrected. This threshold was selected based on experience. The same threshold was used for all test subjects.

After spectrum subtraction, the most probable HR frequency peak was estimated. This is initiated with a proprietary peak detection and selection algorithm. The peak selection starts with the search—in the 8-second window—of the dominant peak frequency around the previous HR estimate frequency. The dominant frequencies that are less than 0.15 Hz (9 BPM) of the prior estimate were chosen. This corresponding window size was selected because a change of 9 BPM is the maximum plausible physiologically difference between two consecutive 8-second windows. If there are no detected peaks in the search window, the estimate of the previous estimation window is chosen. When the peak selection stage chooses the previous estimation result multiple times consecutively, it becomes more probable that the HR has already moved outside the 0.15 Hz

window around the previous HR peak frequency (±9 BPM). To address this problem, the algorithm counts the number of times the previous estimate. If this count is three, the dominant frequency in the whole analysis 8-second window band is chosen as the HR frequency estimate.

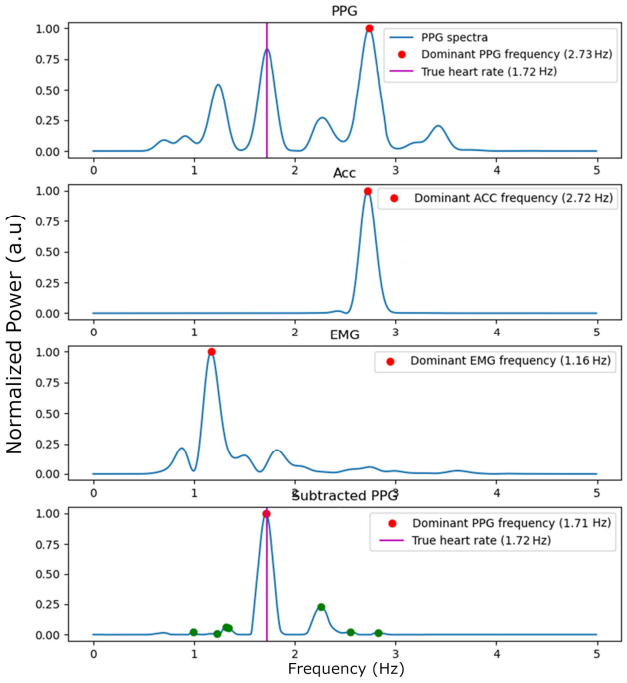

Fig. 3. *Spectrum subtraction example: Corrupted photoplethysmogram (PPG) spectrum (First panel), the acceleration spectrum (second panel), electromyogram (EMG) spectrum (third panel), and the resulting PPG spectrum after the subtraction algorithm (fourth panel). After spectrum subtraction, the true HR frequency is dominant.*

D. Statistical analyses

The HR estimates from the spectrum subtraction algorithm are compared with the reference ECG-based HR using an 8-second estimation window as in the PPG HR. The R-peaks of the ECG are detected, and the RR-intervals are calculated. The reference HR is calculated through the average RR-interval:

$$HR_{ECG} = 60 / \left(\frac{\sum_{i=1}^{N} RR(i)}{N} \right) \quad (9)$$

where HR_{ECG} is the ECG HR estimate, $RR(i)$ is the RR-interval of ith R-peak pair, and N is the number of RR-intervals.

To evaluate the performance of the PPG-based HR estimates, the absolute error (AE) for each estimation window is calculated:

$$AE(i) = |HR_{PPG}(i) - HR_{ECG}(i)| \quad (10)$$

where $AE(i)$ is the absolute error in the window index i, HR_{PPG} is the PPG HR estimate, and HR_{ECG} is the reference gold standard HR using the ECG device.

To measure the general performance, we used the mean absolute error (MAE) and was calculated as:

$$MAE = \frac{\sum_{i=1}^{N} AE(i)}{N} \quad (11)$$

where N is the total number of estimation windows and $AE(i)$ is the AE in the window index i. The spread of *MAEs* measures the accuracy differences between subjects. This is measured the standard deviation of *MAEs:*

$$SdMAE = \sqrt{\frac{\sum_{i=1}^{N} (MAE(i) - MAE_{average})^2}{N}} \quad (12)$$

where $SdMAE$ is the standard deviation of mean absolute errors, N is the number of data subjects, and $MAE_{average}$ is the average of the mean absolute errors of all subjects. The sdMAE is the standard deviation of the MAEs of the subjects for a given task, showing the deviations in accuracy between people.

To measure the precision and spread of the estimates, the standard deviation of the absolute errors (SdAE) for each subject's task. It was calculated as:

$$SdAE = \sqrt{\frac{\sum_{i=1}^{N} (AE(i) - MAE)^2}{N - 1}} \quad (13)$$

The pooled standard deviation of absolute errors ($SdAE_{pool}$) is used to estimate the average spread of data points of different groups around their means. In practice, it is the average of standard deviations of absolute errors for a given task. As the pooled standard deviation is calculated for each independent task containing the same amount of HR estimates each, the equation for pooled standard deviation becomes:

$$SdAE_{pool} = \sqrt{\frac{SdAE_1{}^2 + SdAE_2{}^2 + \cdots + SdAE_N{}^2}{N}} \quad (14)$$

where N is the number of data subjects, and SdAE is the standard deviation of absolute errors of the subject of a given task.

To investigate the statistical significance of the results, a Wilcoxon signed-rank test is used to further analyze the error differences. This is calculated with a SciPy Python library implementation of the Wilcoxon signed-rank test [26]. The changes in estimation errors are considered to be statistically significant if the p-values are under 0.05.

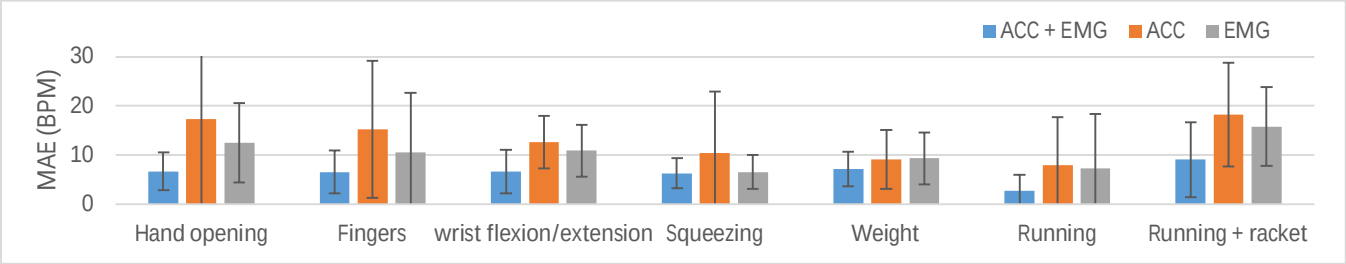

TABLE II
RESULTS USING INDIVIDUAL AND A COMBINATION OF THE ACC AND EMG DURING THE DIFFERENT TASKS.

	Error metrics	Hand opening	Fingers	Wrist flexion / extension	Squeezing	Weight	Running	Running + racket
EMG +ACC	**MAE (BPM)**	6.74	6.60	6.69	6.35	7.18	2.83	9.12
	SdMAE (BPM)	3.81	4.37	4.45	3.10	3.52	3.22	7.60
	$SdAE_{pool}$ (BPM)	8.95	10.02	4.72	7.32	6.60	6.06	8.94
ACC	**MAE (BPM)**	17.33	15.28	12.68	10.38	9.20	8.04	18.29
	SdMAE (BPM)	23.27	13.91	5.33	12.65	6.00	9.74	10.53
	$SdAE_{pool}$ (BPM)	21.32	18.66	12.12	10.83	8.17	11.33	13.49
EMG	**MAE (BPM)**	12.51	10.52	10.94	6.57	9.35	7.33	15.88
	SdMAE (BPM)	8.08	12.22	5.26	3.47	5.22	11.03	7.97
	$SdAE_{pool}$ (BPM)	16.12	14.24	9.40	7.46	8.56	12.17	13.96

MAE: mean absolute error, BPM: beats per minute, **SdMAE**: Standard deviation of MAE, **$SDAE_{pool}$**: standard deviation of the absolute error; **EMG**: electromyography, **ACC**: acceleration.

TABLE III
MAE AND SD IN BPM AND PERCENTAGE CHANGE WHEN ADDING EMG REFERENCE AND ACCELERATION REFERENCE.

Task Δ	Hand opening	Fingers	Wrist flexion / extension	Squeezing	Weight	Running	Running + racket
Δ MAE (BPM)	-10.59	-8.68	-5.99	-4.03	-2.017	-5.21	-9.16
Δ MAE (%)	-61.09	-56.80	-47.27	-38.84	-21.92	-64.82	-50.12
Δ SdMAE (BPM)	-19.46	-9.54	-0.88	-9.55	-2.48	-6.52	-2.93
Δ SdMAE (%)	-83.63	-68.62	-16.48	-75.53	-41.37	-66.93	-27.86
Δ $SdAE_{pool}$ (BPM)	-12.38	-8.63	-7.40	-3.51	-1.57	-5.28	-4.60
Δ $SdAE_{pool}$ (%)	-58.04	-46.27	-61.07	-32.41	-19.25	-46.55	-33.72

MAE: mean absolute error, **BPM**: beats per minute, **SdMAE**: Standard deviation of MAE, **$SDAE_{pool}$**: standard deviation of the Absolute error, **EMG:** electromyography, **ACC**: acceleration**.**

TABLE IV
P-VALUES FOR EACH TASK CALCULATED FROM COMPARISON OF MAES OF USING ONLY ACC REFERENCE AND USING ACC + EMG REFERENCES

	Hand opening	Fingers	Wrist flexion / extension	Squeezing	Weight	Running	Running + racket
p-value	0.027*	0.0039*	0.0039*	0.0078*	0.20	0.012*	0.012*

*** Indicates a significant value ($p \leq 0.05$). EMG:** electromyography, **ACC**: acceleration

TABLE V
P-VALUES FOR EACH SUBJECT FROM ALL TASKS CALCULATED FROM COMPARISON OF MAES OF USING ONLY ACC REFERENCE AND USING ACC + EMG REFERENCES

	Subject1	Subject2	Subject3	Subject4	Subject5	Subject6	Subject7	Subject8	Subject9
p-value	0.031*	0.047*	0.016*	0.58	0.016*	0.16	0.016*	0.047*	0.016*

*** Indicates a significant value ($p \leq 0.05$). EMG:** electromyography, **ACC**: acceleration

III. Results and Discussion

Artifact removal was applied to the measurements taken from the test subjects. For comparison, the algorithm was used with both movement references—EMG and acceleration—individually and with both references combined.

The proposed HR estimation method was tested on two minutes of clear PPG from all subjects. The MAE and $SdAE_{poo}$ were 1.12 and 1.02 BPM, respectively, when compared to the ECG-derived reference HR. This sets the highest possible accuracy to which the other measurements are compared.

Results are shown in Table I and depicted in Fig. 4. The reported MAE values are averages of all subjects from a given task, showing the average performance of the method.

When comparing the results using different movement reference signals, the use of EMG as movement reference improves the HR estimation accuracy. The solution with both EMG and acceleration signals reached the lowest errors in all movement tasks. Also, the deviation between different subjects is smaller.

On average, EMG alone performed better than using only an acceleration signal as a movement reference. This is probably because the accelerometer does not detect tissue movements as reliably as the EMG [13]–[16]. However, even though there is no actual EMG activity, the EMG signal also contains acceleration related artifacts. Nevertheless, the inclusion EMG adds additional and complementary movement artifact information when compared to the accelerometer signal.

In total, there is an average MAE decrease of 5.21 BPM in the running task when EMG is added in addition to the accelerometer as the movement reference. However, closer inspection shows that some subjects exhibited hand muscle activity during their running task, which induced tissue movement artifacts to the PPG signal. Similar observations were noted by Lee et *al*. [16]. As expected, adding a floorball racket to the running measurement introduced more hand muscle activations, which led to worse estimation accuracies.

As seen in Table 3, the percentage decrease in the HR estimation error is significant when EMG is added as a tissue movement reference. The MAE decreased on average by 49%, and the standard deviation of MAE decreased by 54%. In addition, the $SdAE_{pool}$ decreased by 43%. Thus, the general robustness of the HR estimation improved considerably with the addition of the EMG movement reference.

The statistical significance of MAE reduction was investigated by means of calculating p-values for MAE pairs with and without the EMG motion reference. From the p-values in Tables 4 and 5 it can be seen that the p-values are under 0.05 for most tasks, making them statistically significant. Only in the weightlifting task no statistically significant improvement was achieved with p-value of 0.20. This is understandable, as the weightlifting movement is easily detectable with accelerometers and addition of EMG does not provide supplementary information. Also, the results from subjects 4 and 6 are not statistically significant with p-values of 0.58 and 0.16 respectively. This is due to the fact that the EMG signal amplitudes were low compared to the acceleration signal, so that the EMG reference did not provide additional information on the movement artifacts.

In contrast to Silverio et *al*. [14], the EMG was measured from the wrist instead of the forearm, which contains less muscle, leading to smaller amplitude signals. Nevertheless, as seen in Fig. 5, the acceleration and tissue movement artifacts occurring at different frequencies are visible in the spectrograms. The frequency estimates calculated from the acceleration and EMG are marked with blue and orange color, respectively (Fig. 3). While the acceleration can detect the swinging motion of the hand during running, the EMG can detect the muscle contractions of the hand squeezing the floorball racket. The addition of EMG proves to be the most effective when the body movement and tissue movement happen at different frequencies. However, as the statistical test by subject shows, the wrist EMG does not provide statistically significant improvement for all people. Inter subject differences in wrist anatomy and muscle mass can affect the effectiveness of the wrist EMG use as artifact reference.

Despite the effectiveness of the EMG as a reference signal, future work could lead to further improvement. Our algorithm implementation had some shortcomings: First, when there was a low PPG SNR, or the PPG HR-frequency power was weak, the algorithm was not able to recover the PPG HR frequencies, leading to discontinuities in the spectrograms and increasing the MAE. Second, when the artifact and HR frequencies overlapped, the algorithm would subtract the HR frequency as an artifact leading to additional frequency discontinuities in the spectrograms. These discontinuities could be avoided by disabling the spectrum subtraction algorithm when the tracked artifact frequencies overlap with the HR frequencies.

Based on the current study the smart watch EMG could be used to enhance HR estimation in activities involving tissue movements. Implementation of EMG sensing in smart watch form factor would somewhat increase the complexity and the power consumption of the device. However, given the observed benefit in the current study, the implementation challenges could be justifiable .

Finally, the study has the following limitations: subjects' availability led to a small sample. In practice, the use of adhesive electrodes in wristwatches is not feasible. Thus, our results might not match precisely an EMG-equipped wristwatch without adhesive electrodes because these electrodes might have mitigated movement-related artifacts. Also, the present study did not consider irregular movement artifacts, which are relevant in several activities in real use. For being efficiently addressed, irregular movement artifacts most likely require other than frequency domain-based signal processing approaches. The used algorithm considered only frequencies above 0.8 Hz, which disregards heart rates under 48 BPM. This would lead to erroneous estimates to people with HR lower than 48 BPM. Thus, future research is needed.

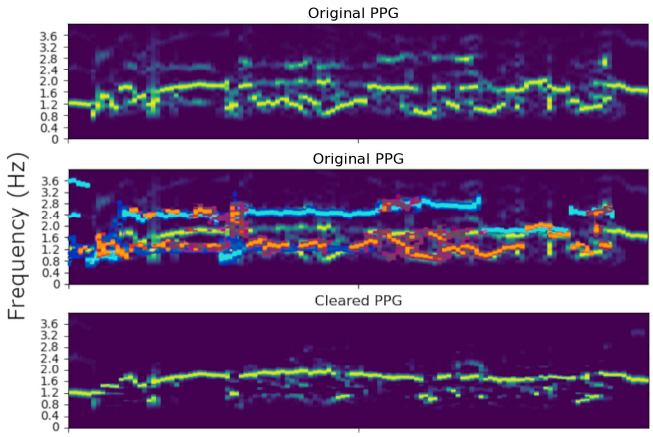

Fig. 5. *Recording of a subject running while holding a racket. Spectrograms of the original photoplethysmogram (PPG) (top panel), the original PPG with acceleration artifact (blue) and tissue movement artifact (orange) (middle panel), and the PPG signal after spectrogram subtraction (bottom panel).*

IV. Conclusion

The use of EMG as a tissue movement reference to improve the HR estimates of a reflective PPG in a wristwatch was investigated. The results indicate that EMG is a specific tissue movement reference and contains additional and complementary information on the PPG artifacts. Furthermore, the addition of both EMG and acceleration in the spectrum subtraction algorithm decreased the estimation error by 49% compared to using only acceleration. EMG thus provides a novel and effective modality for improving the performance of the optical HR estimation from the wrist.

References

[1] E. Boulpaep, "Integrated Control of the Cardiovascular System," in *Medical physiology*, Philadelphia, PA: Elsevier, 2017, pp. 572–587.

[2] B. W. Nelson, C. A. Low, N. Jacobson, P. Areán, J. Torous, and N. B. Allen, "Guidelines for wrist-worn consumer wearable assessment of heart rate in biobehavioral research," *Npj Digital Medicine*, vol. 3, no. 1, p. 90, 2020, doi: 10.1038/s41746-020-0297-4.

[3] V. V. Tuchin and S. J. Matcher, "Handbook of Optical Biomedical Diagnostics, Second Edition, Volume 1: Light-Tissue Interaction," 2016, doi: 10.1117/3.2219603.ch9.

[4] J. Allen, "Photoplethysmography and its application in clinical physiological measurement," *Physiol Meas*, vol. 28, no. 3, pp. R1–R39, 2007, doi: 10.1088/0967-3334/28/3/r01.

[5] A. J. Casson, A. V. Galvez, and D. Jarchi, "Gyroscope vs. accelerometer measurements of motion from wrist PPG during physical exercise," *Ict Express*, vol. 2, no. 4, pp. 175–179, 2016, doi: 10.1016/j.icte.2016.11.003.

[6] A. Temko, "Estimation of heart rate from photoplethysmography during physical exercise using Wiener filtering and the phase vocoder," *2015 37th Annu Int Conf Ieee Eng Medicine Biology Soc Embc*, vol. 2015, pp. 1500–1503, 2015, doi: 10.1109/embc.2015.7318655.

[7] A. Temko, "Accurate Heart Rate Monitoring During Physical Exercises Using PPG," *Ieee T Bio-med Eng*, vol. 64, no. 9, pp. 2016–2024, 2017, doi: 10.1109/tbme.2017.2676243.

[8] K. R. Arunkumar and M. Bhaskar, "CASINOR: Combination of adaptive filters using single noise reference signal for heart rate estimation from PPG signals," *Signal Image Video Process*, vol. 14, no. 8, pp. 1507–1515, 2020, doi: 10.1007/s11760-020-01692-6.

[9] S. Hanyu and C. Xiaohui, "Motion Artifact Detection and Reduction in PPG Signals Based on Statistics Analysis," *2017 29th Chin Control Decis Conf Ccdc*, pp. 3114–3119, 2017, doi: 10.1109/ccdc.2017.7979043.

[10] A. Reiss, I. Indlekofer, P. Schmidt, and K. V. Laerhoven, "Deep PPG: Large-Scale Heart Rate Estimation with Convolutional Neural Networks," *Sensors*, vol. 19, no. 14, p. 3079, 2019, doi: 10.3390/s19143079.

[11] D. Pollreisz and N. TaheriNejad, "Detection and Removal of Motion Artifacts in PPG Signals," *Mob Networks Appl*, vol. 27, no. 2, pp. 728–738, 2022, doi: 10.1007/s11036-019-01323-6.

[12] H. Chung, H. Ko, H. Lee, and J. Lee, "Deep Learning for Heart Rate Estimation From Reflectance Photoplethysmography With Acceleration Power Spectrum and Acceleration Intensity," *Ieee Access*, vol. 8, pp. 63390–63402, 2020, doi: 10.1109/access.2020.2981956.

[13] Y. Zhang *et al.*, "Motion Artifact Reduction for Wrist-Worn Photoplethysmograph Sensors Based on Different Wavelengths," *Sensors Basel Switz*, vol. 19, no. 3, p. 673, 2019, doi: 10.3390/s19030673.

[14] A. A. Silverio *et al.*, "Micromotion Artefact Reduction of a Wrist Worn PPG Sensor Using Green Light PPG and Surface EMG," *2020 Ieee 8th R10 Humanit Technology Conf R10-htc*, vol. 00, pp. 1–5, 2020, doi: 10.1109/r10-htc49770.2020.9356956.

[15] N. D. P. Ferreira, C. Gehin, and B. Massot, "Ambient Light Contribution as a Reference for Motion Artefacts Reduction in Photoplethysmography," *Proc 13th Int Jt Conf Biomed Eng Syst Technologies*, pp. 23–32, 2020, doi: 10.5220/0008878800230032.

[16] H. Lee, H. Chung, J.-W. Kim, and J. Lee, "Motion Artifact Identification and Removal from Wearable Reflectance Photoplethysmography Using Piezoelectric Transducer," *Ieee Sens J*, vol. 19, no. 10, pp. 3861–3870, 2019, doi: 10.1109/jsen.2019.2894640.

[17] Salehizadeh, S.M.A., D. Dao, J. Bolkhovsky, C. Cho, Y. Mendelson, and K.H. Chon. A novel time-varying spectral filtering algorithm for reconstruction of motion artifact cor-rupted heart rate signals during intensive physical activities using a wearable photople-thysmogram sensor, Sensors, 16, PMID 26703618, 2015.

[18] Kong, Y., and K.H. Chon, Heart rate tracking using wearable photoplethysmographic sen-sor during treadmill exercise, IEEE Access, 7:152421-152428, 2019.

[19] "Mentalab Explore ExG device." https://mentalab.com/product (accessed Jun. 17, 2022).

[20] "Ambu Whitesensor ECG electrode." https://www.ambu.com/cardiology/ecg-electrodes/product/ambu-whitesensor-4500m-h (accessed Jun. 17, 2022).

[21] N. Sviridova, T. Zhao, K. Aihara, K. Nakamura, and A. Nakano, "Photoplethysmogram at green light: Where does chaos arise from?," *Chaos Solitons Fractals*, vol. 116, pp. 157–165, 2018, doi: 10.1016/j.chaos.2018.09.016.

[22] W. Guo, X. Sheng, H. Liu, and X. Zhu, "Development of a Multi-Channel Compact-Size Wireless Hybrid sEMG/NIRS Sensor System for Prosthetic Manipulation," *Ieee Sens J*, vol. 16, no. 2, pp. 447–456, 2016, doi: 10.1109/jsen.2015.2459067.

[23] "SciPy Fast Fourier Transform function." https://docs.scipy.org/doc/scipy/reference/generated/scipy.fft.fft.html (accessed Jun. 17, 2022).

[24] J. W. Cooley and J. W. Tukey, "An algorithm for the machine calculation of complex Fourier series," *Math Comput*, vol. 19, no. 90, pp. 297–301, 1965, doi: 10.1090/s0025-5718-1965-0178586-1.

[25] J. M. de Carvalho, "Discrete-Time Signal Transforms," in *Digital Signal Processing*, Momentum Press, 2019.

[26]"SciPyWilcoxon signed rank test."). https://docs.scipy.org/doc/scipy/reference/generated/scipy.stats.wilcoxon.html. (accessed Oct. 1, 2022).

Severi Friman received his M.Sc. (Tech.) degree in electrical engineering from Tampere University, Tampere Finland 2022. Currently he is working as a biosignal detection and processing engineer at Device Concept Laboratories of Finland Research Center, Huawei Technologies Co.,Ltd., Finland. His current research interests are at developing new wearable technologies for health monitoring applications and their use on devices available for general public.

Antti Vehkaoja received his D.Sc. (Tech.) degree in automation science and engineering from Tampere University of Technology, Tampere, Finland in 2015. He is currently an Associate Professor (tenure tract) of Sensor Technology and Biomeasurements at the Faculty of Medicine and Health Technology, Tampere University, Finland. His current research interests include embedded measurement technologies for physiological monitoring and related signal processing and data analysis methods. He has authored more than 100 scientific articles in the field

of biomedical engineering, most of which dealing with physiological measurements.

Jose Maria Perez-Macias received his MS in Biomedical Engineering in Chalmers University of Technology, Gothenburg, Sweden, and MS Telecommunications Engineering in European University of Madrid, Spain. He is currently a PhD student in Biomedical Engineering program in the Faculty of Medicine and Health Technology, Tampere University, Finland. His current research interests include wearable signal processing and machine learning in film-type mattress signal analysis for breathing and heart diagnosis (ballistocardiography), sleep estimation, EEG analysis in intensive care units, and wearable product concept development.